

### **OPEN ACCESS**

EDITED BY Alexandra Gemitzi,

Democritus University of Thrace, Greece
REVIEWED BY

Yonaxin Ni.

Yellow River Institute of Hydraulic Research,

China

Yanyu Dai,

China University of Mining and Technology,

\*CORRESPONDENCE Wenxin Li ⋈ 18153999308@163.com

RECEIVED 16 July 2025 ACCEPTED 19 August 2025 PUBLISHED 10 September 2025

### CITATION

Li W, Chen P, Li K and Shu H (2025) Exploring runoff variation and attribution analysis based on the SWAT model and the Budyko framework in the Huangyang River of the Northwest Inland Region, China. *Front. Water* 7:1667387. doi: 10.3389/frwa.2025.1667387

### COPYRIGHT

© 2025 Li, Chen, Li and Shu. This is an open-access article distributed under the terms of the Creative Commons Attribution License (CC BY). The use, distribution or reproduction in other forums is permitted, provided the original author(s) and the copyright owner(s) are credited and that the original publication in this journal is cited, in accordance with accepted academic practice. No use, distribution or reproduction is permitted which does not comply with these terms.

# Exploring runoff variation and attribution analysis based on the SWAT model and the Budyko framework in the Huangyang River of the Northwest Inland Region, China

Wenxin Li1\*, Peng Chen1, Kuijing Li2 and Heping Shu2

<sup>1</sup>Construction Cost and Fee Management Center of Water Conservancy Projects, SLT.GANSU.GOV. CN, Lanzhou, China, <sup>2</sup>College of Water Conservancy and Hydropower Engineering, Gansu Agricultural University, Lanzhou, China

The ecological degradation and groundwater level decline caused by runoff reduction in arid inland river basins are becoming increasingly severe under the dual pressures of global climate change and human activities. The Huangyang River was selected as the study area, the Mann-Kendall mutation test and sliding T-test method were used to identify runoff mutation points. The transfer matrix method and sensitivity analysis were applied to clarify the relationship between land use change and runoff variation. The Budyko water-heat coupling theory and the SWAT model were carried out to explore the driving mechanisms of climate change and human activities on runoff. The results showed that the annual runoff decreased significantly at a rate of  $0.042 \times 10^8 \,\mathrm{m}^3 \cdot \mathrm{a}^{-1}$  (p < 0.05), with 1991 being the mutation point. From the baseline period to the change period, runoff decreased by  $0.15 \times 10^8$  m $^3$ . The attribution analysis of the SWAT model and the Budyko hypothesis consistently indicates that human activities were the main drivers of runoff changes, with human activities contributing 69.52 and 68.84%, and climate change contributing 30.48 and 31.16%, respectively, among them, the contribution rate of land use was 10.70%, and that of other human activities was 58.82%. This confirms that human activities have significantly altered the hydrological processes of the basin. The findings provide theoretical support for the sustainable development of inland river basins.

KEYWORDS

SWAT model, Budyko hypothesis, attributional analysis, land use, arid and semi-arid basins

### 1 Introduction

Under the dual pressures of global climate change and intensified human activities, aridzone ecosystems are facing increasingly severe challenges, including ecological degradation and water resource scarcity (Liu C. X. et al., 2022). As critical water sources in arid regions, inland rivers play a vital role in sustaining oases, recharging groundwater, and preventing desertification. Consequently, variations in river runoff have become key limiting factors for regional ecological security (Jun et al., 2022; Zhou et al., 2019). The Huangyang River, located on the northern slope of the eastern Qilian Mountains, serves as a major water conservation area in the central Hexi Corridor and is a primary tributary of the Shiyang River Basin.

Changes in its runoff directly affect the stability of downstream oases and ecosystems. In recent years, the basin has experienced a notable decline in runoff, degradation of oasis areas, and over-extraction of groundwater—posing serious challenges to regional water resource management and ecological restoration (Wu Z. Q. et al., 2022). Therefore, identifying and quantifying the relative contributions of climate change and human activities to runoff variation is of critical importance for sustainable development and watershed governance in this fragile environment.

Existing studies generally suggest that climatic factors, especially reduced precipitation and enhanced potential evapotranspiration, are the main natural drivers of runoff reduction (He et al., 2017; Yuan et al., 2018). The climate in arid areas shows greater instability and extremity. Especially in the Qilian Mountain area where the Huangyang River is located, the interannual precipitation fluctuation and temperature increase significantly increase the evapotranspiration flux and weaken the infiltration and confluence efficiency of water resources (Yao et al., 2015). However, the intervention paths of human activities on hydrological processes are more complex and diverse, involving ecological engineering measures such as land use change, water conservancy infrastructure construction, groundwater extraction and returning farmland to forest (Chen et al., 2014; Wang et al., 2024). Among them, the vegetation restoration caused by the policy of returning farmland to forest significantly increased the surface coverage of the basin, increased soil water retention and evapotranspiration water consumption, and changed the surface runoff generation path and water distribution to a certain extent (Feng et al., 2025). Especially in the middle and upper reaches with a relatively steep slope, while artificial vegetation restoration promotes ecological improvement, it also significantly weakens the available runoff downstream (Lan et al., 2021). Wang L. et al. (2019) used the SWAT model to evaluate the runoff response under different land use scenarios in the upper reaches of the Huangyang River and found that grassland degradation and the expansion of irrigated area were the main reasons for the reduction of runoff in the basin. Liu et al. (2021) constructed a SWAT sub-model in the nested system of the Shiyang River—Huangyang River Basin to simulate the impact of oasis irrigation on runoff and groundwater in the basin, and found that the dominant role of human activities was significantly higher than that of climatic factors. Duan (2023) estimated the attribution of runoff changes in the Huangyang River Basin since 2000 based on the Budyko framework, and believed that human activities (such as land use changes) contributed as much as 72%, among which the increase in evapotranspiration caused by vegetation restoration was the main mechanism.

Currently, the mainstream methods for attributing runoff changes include time series comparison, double mass curve (DMC) analysis, Budyko hydro-thermal coupling frameworks, and physically-based hydrological modeling. The DMC method is simple to implement but lacks the capacity to adequately capture nonlinear relationships (Nalley et al., 2019). The Budyko hypothesis, which characterizes climate and anthropogenic influences through the aridity index and vegetation parameter (n), has been widely applied in attribution studies in semi-arid regions (Duan, 2023; He et al., 2019). However, the Budyko framework simplifies surface hydrological processes and has limited ability to represent the spatial heterogeneity of land use change. In contrast, distributed hydrological models such as SWAT can integrate multiple factors, such as climate, topography, and land use, that offering stronger representation of physical mechanisms (Si

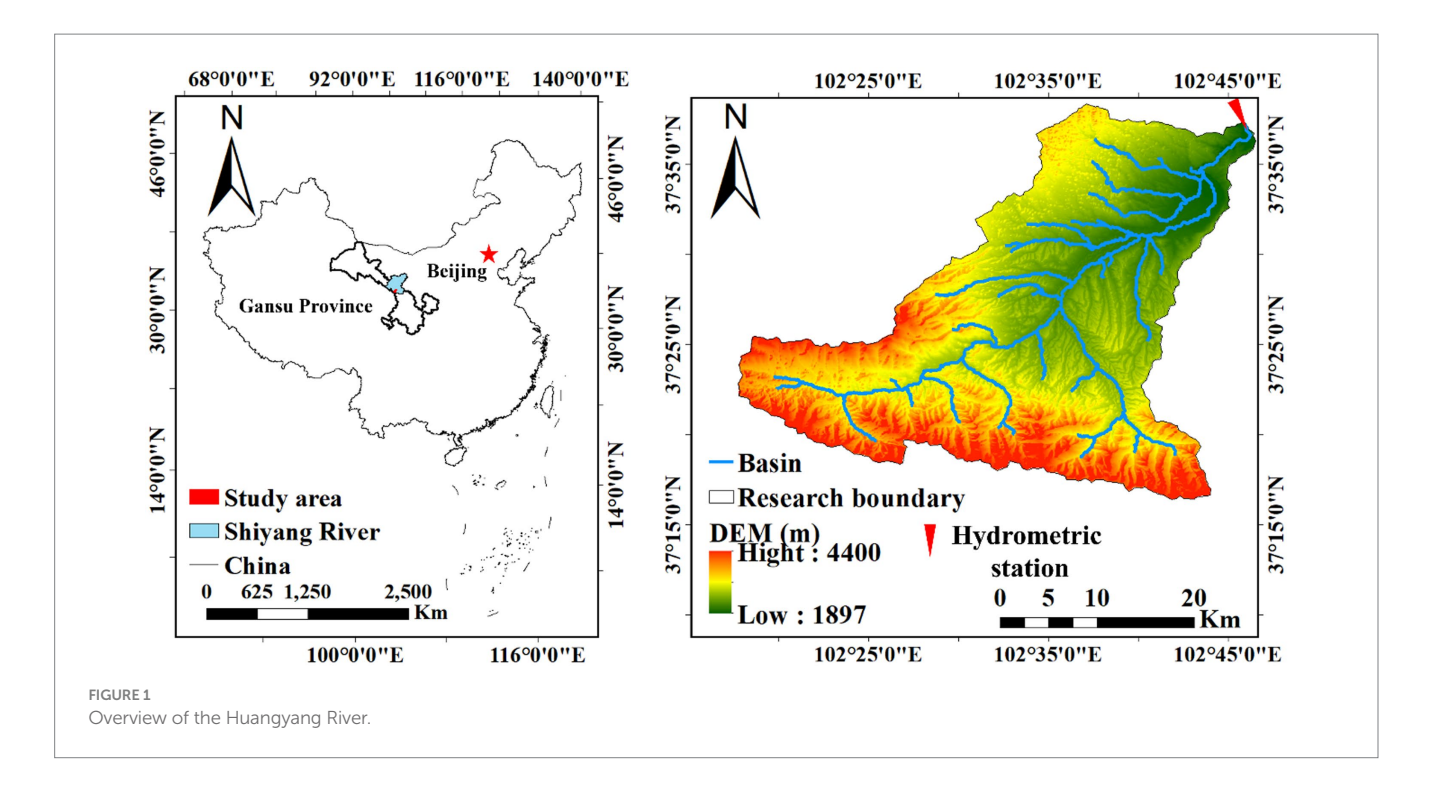
et al., 2025; Hu et al., 2021). For example, Hu et al. (2020) combined SWAT simulations with the Budyko approach to achieve dual attribution of evapotranspiration and runoff. Wang et al. (2023) employed SWAT and CMIP5 climate projections to explore future runoff trends in inland river basins. The SWAT model demonstrates high adaptability in multi-scale hydrological response studies in arid regions. However, its parameter calibration process is complex and subject to uncertainties, necessitating the use of tools such as SWAT-CUP for sensitivity analysis and optimization (Zhao et al., 2023). Although previous studies have attempted to combine the Budyko framework with SWAT modeling, most remain limited to result comparisons between the two approaches. There has been little exploration of their complementary strengths in attribution, and few studies have examined the cascading feedback mechanisms among climate, vegetation, and hydrology in arid basins. Therefore, this study takes the Huangyang River Basin as a representative case to establish an integrated framework of "SWAT simulation-vegetation feedback-Budyko attribution" in order to clarify the driving mechanisms behind runoff changes under different scenarios. It also aims to quantify the contributions of various land use changes to runoff variability, thereby addressing the current limitations in process coupling and synergistic analysis.

Therefore, taking the Huangyang River Basin as the research object and integrating multi-source remote sensing data, distributed hydrological modeling, and the Budyko water-heat coupling theory, the research objectives are as follows: (1) precisely identify the mutation characteristics of runoff series by combining the Mann-Kendall mutation test and the sliding T-test, and establish a temporal correlation of climate change-land use-runoff response; (2) use a complementary strategy of the Budyko elasticity coefficient method and SWAT scenario simulation to quantitatively separate the contribution rates of climate change and human activities as multiple driving factors; (3) construct a land use transfer matrix and hydrological sensitivity coupling model to reveal the vegetation-runoff feedback mechanism driven by the "Grain for Green" policy. The research results can provide theoretical support for the collaborative management of "water resources-ecosystem-socio-economy" in arid regions and offer scientific basis for adaptive water resource management in these areas.

### 2 Materials and methods

### 2.1 Study area

The Huangyang River Basin (102.04°–102.75°E, 37.57°–37.63°N) is a component of the Shiyang River water system, and the two form a hydrological unit that "partially supports the whole" (Figure 1). Spans the Liangzhou District of Wuwei City, and the Tianzhu Tibetan Autonomous County in Gansu Province. Its source is located along the northern slope of the eastern end of the Qilian Mountains, the river source elevation is 4,200 m, and the basin mainly develops two primary tributaries, the Haxi River and the Xiamen River. The two main tributaries converge above Xiejiahe Bay with the Jiadaogou stream to form the mainstream, which also receives intermittent tributaries like Sigou, Dahonggou, and Daxigou before flowing into the Huangyang Reservoir. The length of the main river above the reservoir is 34.89 km, with a catchment area of 753 km² in Gansu Province. The river's gradient is 29.7‰, and it flows in a southwest to northeast direction.



Both banks of the river are characterized by high mountains. The upper reaches have abundant grassland, forest coverage, and good vegetation. The middle reaches also have grassland and forests in some areas, while the lower reaches have farmland and barren hills with exposed loess, poor vegetation, and eroded soil. The soils in the upper reaches are mainly mountain brown soils and subalpine meadow soils, while the middle and lower reaches have oasis irrigation soils and gray desert soils.

### 2.2 Data source

The dataset includes: DEM data with a 30 m spatial resolution; Monthly runoff and precipitation data (1956–2023) from the Huangyang River Reservoir Station; Daily meteorological data (1956–2023), including precipitation, temperature, humidity, and wind speed, from Xiamenkou, Haxi, Mozi Zui, and Huangyang River Reservoir stations; Basin-wide average potential evapotranspiration data at the county level; Land use data for 1980, 1990, 2000, 2010, and 2020 (Table 1).

### 2.3 Methods

# 2.3.1 Mann-Kendall non-parametric change point test method

The Mann-Kendall change point test method is recommended by the World Meteorological Organization for detecting change points in runoff caused by meteorological factors and other variables (Praveen et al., 2020). The MATLAB 2023b was used to solve for the values of  $UF_k$  and  $UB_k$ , UF and UB curve plots are drawn. When the UF value is positive, the sequence shows an increasing trend, while a negative UF value indicates a decreasing trend. If the UF and UB curves intersect and the intersection point lies within the significance level range ( $\alpha = 0.05$ , with a critical value of  $U_\alpha = \pm 1.96$ ), the corresponding

TABLE 1 Data sources.

Data type	Data description	Data source
Climate data	Daily precipitation, wind speed, relative humidity, sunshine hours, average/minimum/maximum temperature from 1956 to 2023.	China National Meteorological Information Cente (https://www.nmic. cn/)
Soil data	The attributes of the world soil database (HWSD) soil spatial data	National Cryosphere Desert Data Center (http://www.ncdc.ac. cn/portal)
Land use data	Land use remote sensing monitoring data for the years 1980, 1990, 2000, 2010, and 2020 (30 m)	Remote sensing image interpretation of data by the Chinese Academy of Sciences (https://www.resdc.cn/)
Runoff data	Monthly data of Huangyanghe reservoir station from 1956 to 2023	"Yellow River Hydrological Yearbook" and Hydrological Station
Potential evapotranspiration data	Daily and monthly data from 1956 to 2023	China National Meteorological Information Cente (https://www.nmic. cn/)
DEM data	30 m spatial resolution elevation data	Geospatial data cloud of the Chinese Academy of Sciences (http://www.gscloud. cn)

time of the intersection is considered the change point. This method is mainly used to identify runoff change points in the study. The sliding T-test method is used to detect change points in continuous hydrological data sequences, and it is more stable, particularly in the presence of outliers and skewed data.

### 2.3.2 Budyko hypothesis method

The Budyko hypothesis theory is a convenient and effective tool for analyzing the water-energy balance of a watershed (Kim and Chun, 2021). There are many control equations for the Budyko hypothesis, and different theoretical and empirical equations have improved the Budyko framework. Choudhury and Yang derived other functions related to rainfall, runoff, and underlying surface characteristics, which can more universally and effectively determine model parameters. The derived formulas are as follows (Choudhury, 1999; Yang et al., 2008).

$$R = P - \frac{PET0}{\left(P^n - ET0^n\right)^{1/n}} \tag{1}$$

Where P is the observed annual average precipitation; R is the runoff depth; n comprehensively reflects the characteristics of the watershed's underlying surface, and the parameter n can be calculated using MATLAB software from this equation. Assuming that P, PET, and n are independent of each other, the total differential of R with respect to each factor is:

$$dR = \frac{\partial R}{\partial P}dR + \frac{\partial R}{\partial PET}dPET + \frac{\partial R}{\partial n}dn$$
 (2)

The elasticity coefficient can be expressed as:

$$\varepsilon_{xi} = \frac{\partial R}{\partial x_i} \times \frac{x_i}{R}$$
 (3)

Where  $\varepsilon_{xi}$  represents the elasticity of runoff with respect to P, PET, and n, respectively. Therefore, Equation 2 simplifies to:

$$dR = \epsilon_{xp} \frac{R}{x_p} dx_p + \epsilon_{xPET} \frac{R}{x_{PET}} dx_{PET} + \epsilon_{xn} \frac{R}{x_n} dx_n \tag{4} \label{eq:dR}$$

The calculation of the elasticity coefficients of runoff is as follows:

$$\varepsilon_{p} = \frac{1 - \left[ \frac{\left( \text{PET/P} \right)^{n}}{1 + \left( \text{PET/P} \right)^{n}} \right]^{1/n + 1}}{1 - \left[ \frac{\left( \text{PET/P} \right)^{n}}{1 + \left( \text{PET/P} \right)^{n}} \right]^{1/n}}$$
 (5)

$$\varepsilon_{\text{PET}} = \frac{1}{1 + (\text{PET/P})^{n}} \frac{1}{1 - \left[\frac{(\text{PET/P})^{n}}{1 + (\text{PET/P})^{n}}\right]^{1/n}}$$
(6)

$$\varepsilon_{n} = \frac{\frac{P^{n} \operatorname{In}(P) + \operatorname{PET} \times \operatorname{In}(\operatorname{PET})}{P^{n} + \operatorname{PET}} - \frac{\operatorname{In}(P^{n} + \operatorname{PET}^{n})}{n}}{\left[1 + \left(\operatorname{PET}/P\right)^{n}\right]^{1/n} - 1}$$
(7)

The calculation of the contribution rate of runoff change (Liu W. L. et al., 2022):

$$\Delta R = R_2 - R_1 \tag{8}$$

$$\Delta P = P_2 - P_1 \tag{9}$$

$$\Delta ET0 = ET0_2 - ET0_1 \tag{10}$$

$$\Delta n = n_2 - n_1 \tag{11}$$

The calculation of runoff depth changes caused by each driving factor:

$$\Delta R_i = \varepsilon_i \frac{R}{i} \Delta i \tag{12}$$

The runoff change caused by each influencing factor is obtained from the water–heat coupling balance equation, and the total runoff depth change is calculated:

$$\Delta R' = \Delta R_P + \Delta R_{ET0} + \Delta R_n \tag{13}$$

Subscripts 1 and 2 represent the reference period and the change period based on the mutation point. The contribution rate is:

$$C_{x} = \frac{\Delta R_{x}}{\Delta R} \times 100\% \tag{14}$$

Subscripts 1 and 2 represent the reference period and the change period in the formula.  $\Delta P$  and  $\Delta PET$  are the changes in precipitation and potential evapotranspiration from the reference period to the change period, in mm;  $\Delta R_P$ ,  $\Delta R_{ET0}$ , and  $\Delta R_n$  represent the runoff changes caused by precipitation, potential evapotranspiration, and land surface changes due to human activities, in mm.

### 2.3.3 Transition matrix

In the study, six land use types were selected for analysis using ArcMap. The detailed process is referenced from the study by Liu et al. (2005). The principle of the transition matrix is as follows:

$$A = (a_{ij})_{n \times n} = \begin{bmatrix} a_{11} & \dots & a_{1n} \\ \dots & \dots & \dots \\ a_{n1} & \dots & a_{nn} \end{bmatrix}$$
 (15)

The  $a_{ij}$  represents the area of land use type in the formula, i and j are the land use types before and after the transition, and n is the total number of land use types.

### 2.3.4 Sensitivity analysis

The sensitivity of the two is expressed using the elasticity relationship based on the relationship between runoff variation and land use. A sensitivity coefficient greater than 1 indicates that a small change in the independent variable causes a larger change in the dependent variable. In other words, the smaller the change in land use type, the greater the change in runoff. Conversely, if the land use change is not sensitive to runoff variation (Zhao et al., 2025).

$$S_{ij} = \left| \frac{(R_{i+1} - R_i) / R_i}{(L_{(i+1)j} - L_{ij}) / L_{ij}} \right| = \left| \frac{\Delta R_i / R_i}{\Delta L_{ij} / L_{ij}} \right|$$
(16)

 $S_{ij}$  is the sensitivity coefficient of runoff in stage i relative to land use type j in the formula,  $R_{i+1}$  and  $R_i$  are the runoff at stages i+1 and i, respectively, and  $L_{(i+1)j}$  and  $L_{ij}$  are the land use types j influencing runoff variation at stages i+1 and i.

### 2.3.5 SWAT hydrological modeling method

The SWAT model is an improved and developed version of the SWRRB model. Due to its basis in physical processes, watershed scale, and continuous time distributed hydrological modeling, it is widely used in fields such as long-term hydrological simulation, non-point source pollution, and sediment variation (Arnold et al., 1998; Raffar et al., 2022). The model considers the spatiotemporal heterogeneity of climate change (daily precipitation, daily temperature) and underlying surface conditions (land use, soil characteristics), quantifying the impacts of climate change and human intervention on runoff. It is applicable to watersheds of various sizes and complexities and can elucidate the detailed processes from precipitation to runoff (Raihan et al., 2020).

The entire study period from 1956 to 2023 is divided into two sequences based on the change points, it was the baseline period and the change period. The SWAT model is used to simulate runoff, and the quantitative separation of the impacts of vegetation cover and climate change on runoff variation is carried out using the following formula. The contribution rates of climate change and human activities to runoff are quantitatively separated through the simulation-observation comparison method, and the calculation formula is as follows:

$$\Delta R = R_2 - R_1 \tag{17}$$

$$\Delta R = R_C + R_H \tag{18}$$

$$\Delta R_C = R_2^{sim} - R_3^{sim} \tag{19}$$

$$\eta_C = \frac{\Delta R_C}{\Delta R} \times 100\% \tag{20}$$

$$\eta_H = \frac{\Delta R_H}{\Delta R} \times 100\% \tag{21}$$

The annual average runoff for the baseline period and the change period are  $R_1$  and  $R_2$ , respectively;  $\Delta R$  represents the change in the

annual average runoff;  $R_C$  and  $R_H$  represent the changes in annual average runoff caused by climate change and human activities, respectively;  $R_2^{sim}$  and  $R_3^{sim}$  The simulated runoff representing the unchanged and changed land use during the change period respectively;  $\eta_C$  and  $\eta_H$  represent the contribution rates of climate change and human activities to the runoff changes.

# 2.3.6 The evaluation indicators of hydrological models

The results exported from the SWAT model are used as input files for the SWAT-CUP software (Abbaspour et al., 2015). During the simulation process, the monthly runoff data from the Huangyanghe Reservoir station are selected for calibration and validation. After conducting sensitivity analysis on the selected parameters using the SUFI-2 algorithm in SWAT-CUP, highly sensitive parameters are screened for the preliminary simulation, and the calibrated optimal parameter values are directly used for validation in the later stage. In the study, two indicators, the coefficient of determination (R²) and the Nash-Sutcliffe efficiency (NSE), are used to evaluate the model simulation results. According to the evaluation criteria in Jiang et al. (2024) (Table 2), the performance of the model can be assessed.

Calculation formula:

$$R^{2} = \frac{\left[\sum_{i=1}^{n} (Q_{s,i} - \bar{Q}_{s})(Q_{m,i} - \bar{Q}_{m})\right]^{2}}{\sum_{i=1}^{n} (Q_{s,i} - \bar{Q}_{s})^{2}(Q_{m,i} - \bar{Q}_{m})^{2}}$$
(22)

NES = 
$$1 - \frac{\sum_{i=1}^{n} (Q_{m,i} - \overline{Q}_{s,i})^{2}}{\sum_{i=1}^{n} (Q_{m,i} - \overline{Q}_{m})^{2}}$$
 (23)

In the formula,  $Q_{s,i}$  represents the simulated runoff, m³/s;  $Q_{m,i}$  represents the measured runoff;  $\overline{Q}_m$  represents the average measured runoff, m³/s;  $\overline{Q}_s$  represents the average simulated runoff, m³/s; i represents the length of the simulated time series.

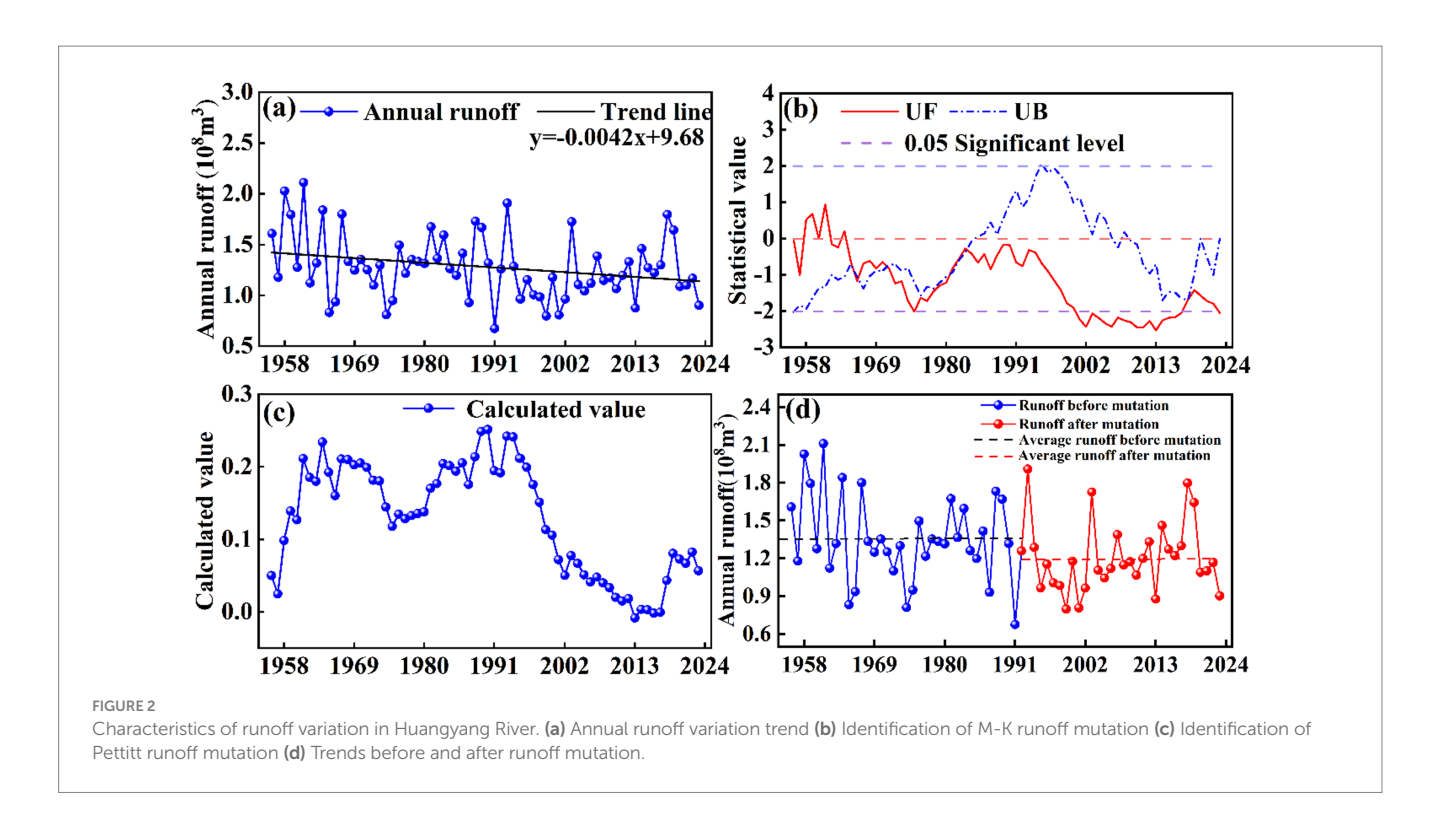
### 3 Results

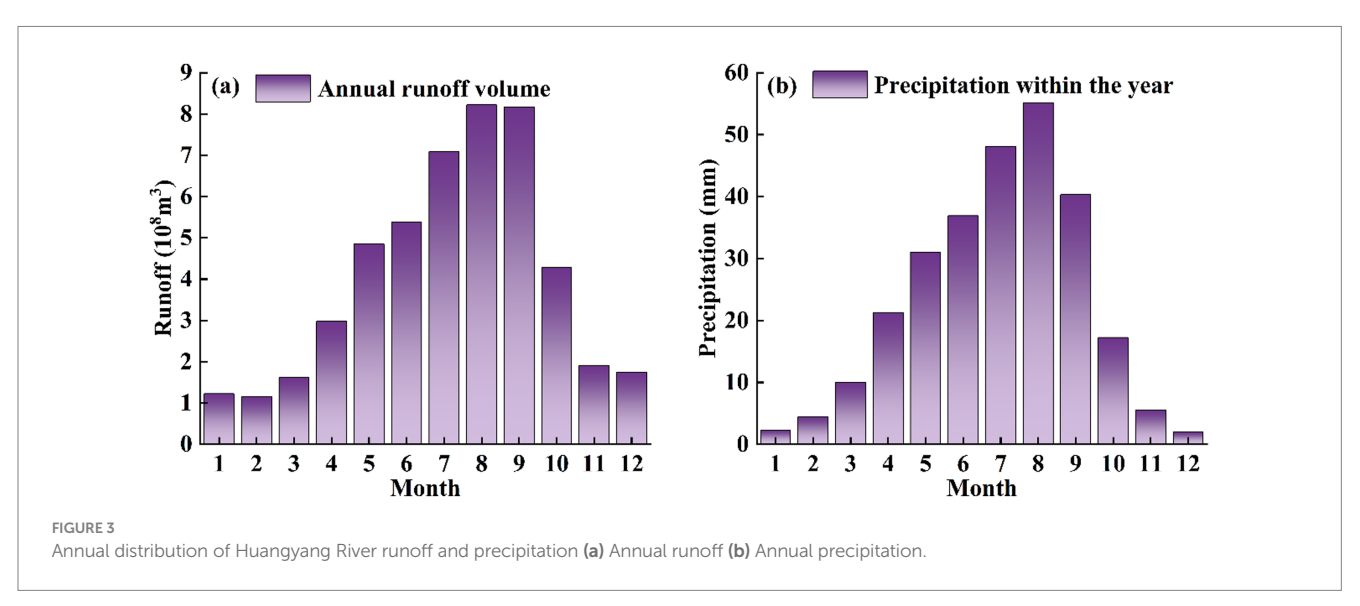
# 3.1 Results of trend and abrupt change testing for annual runoff series of the watershed

The annual runoff at the Huangyang River Reservoir station decreased significantly at a rate of  $-0.042 \times 10^8 \, \text{m}^3/10 \text{a}$  (p < 0.05) (Figures 2, 3). The multi-year average runoff was  $1.28 \times 10^8 \, \text{m}^3$ , with the maximum value of  $2.11 \times 10^8 \, \text{m}^3$  reached in 1961 and the

TABLE 2 Model accuracy evaluation criteria.

Result evaluation	NSE	R <sup>2</sup>	PBLAS		
Excellent	0.75 < NSE ≤ 1	$R^2 > 0.85$	PBLAS < ±10		
Good	$0.65 < NSE \le 0.75$	$0.75 < R^2 \le 0.85$	$\pm 10 \le PBLAS \le \pm 15$		
Qualified	$0.50 < \text{NSE} \le 0.65$	$0.5 < R^2 \le 0.75$	$\pm 15 \le PBLAS \le \pm 25$		
Unreliable	NSE ≤ 0.50	$R^2 \le 0.50$	PBLAS ≥ ±25		





minimum value of  $0.67 \times 10^8$  m³ in 1991. The highest average runoff occurred in the summer, followed by autumn and spring, with winter being the lowest (Figure 4). Regression analysis showed that, before 2000, there was a decreasing trend in spring, summer, and autumn, with the rates of decline being -0.84, -1.10, and  $-0.10 \times 10^8$  m³/10a, respectively. After 2000, the decline slowed down. The overall decreasing trend eased in 2000, and a gradual increasing trend began to emerge, with winter increasing at a rate of  $0.40 \times 10^8$  m³/10a over the entire period. These phenomena suggest that human activities (i.e., the "Grain for Green" project), were implemented after 2000, had a significant impact on the interception of surface runoff.

The increase in winter runoff in the Huangyang River Basin is a typical result of "natural process domination and intensified human regulation." Global warming has led to the degradation of permafrost in the Qilian Mountains. The permafrost, like a "sponge," absorbs more summer precipitation, forming underground water storage, and slowly releases it in winter to replenish the rivers (Li L. et al., 2025). Studies show that the contribution rate of groundwater in the active permafrost layer to the runoff emerging from the Huangyang River is approximately 9%, and its release has significant seasonal lag characteristics (Li et al., 2017).

The M-K method was used to conduct a mutation test on the time series of annual runoff at Huangyang River Reservoir Station from 1956 to 2023 (Figure 3). The M-K test results showed (Figure 2b) that the runoff underwent a change in 1981, while the sliding T-test and cumulative departure method detected a change in 1991 (Table 3). the research sequence was divided into two time periods: 1956–1991 (before mutation) and 1992–2023 (after mutation), and the differences in annual

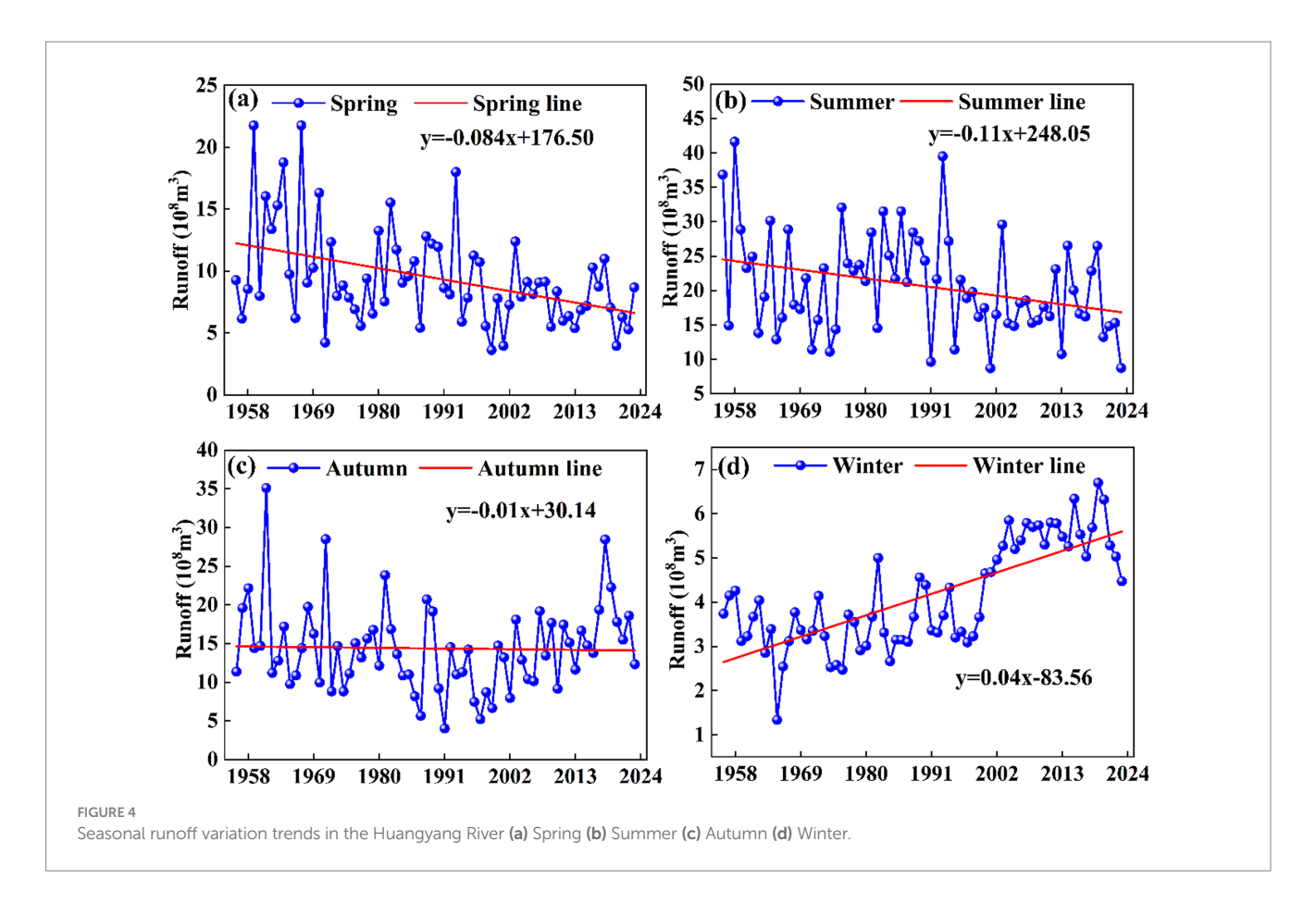


TABLE 3 Runoff change point results for the Huangyang River.

Methods	Change point year	Significance
Mann-Kendall	1981	p < 0.05
Sliding T-test	1991	<i>p</i> = 0.002
Cumulative departure method	1991	Subjective judgment

runoff volume before and after the mutation were analyzed (Figure 2d). The results show that the average annual runoff volume before the mutation is greater than the multi-year average runoff volume. The annual average runoff volume after the mutation is less than the multi-year average runoff volume. The total runoff before and after the sudden change accounted for 55.91 and 44.09% of the total annual runoff respectively, and the average annual runoff before and after the sudden change was approximately the same, the runoff in the change period decreased by  $0.15\times10^8\,\mathrm{m}^3$ , the reduction in runoff volume at Huangyang River Reservoir Station after the sudden change is not significant.

# 3.2 Calibration and validation of the SWAT model

The simulation was conducted based on the detected mutation years (Table 2). Sensitivity analysis was performed using 28 parameters selected according to previous studies, and the sensitivity ranking was determined based on the p-value statistics. After more than 2,000 iterations, 15 parameters were found to have a significant impact on the results (Table 4). The parameters with the strongest sensitivity

were CH\_K2 (channel effective hydraulic conductivity), ALPHA\_BF (baseflow coefficient), SMTMP (snowmelt base temperature), and SFTMP (snowfall temperature). This indicates that the surface runoff process and snowmelt process have a significant impact on the runoff. CH\_K2 (channel effective hydraulic conductivity) and ALPHA\_BF (baseflow coefficient) were found to be the most sensitive, meaning runoff variations are significantly influenced by surface runoff processes, followed by snowmelt changes, suggesting that runoff variations are mainly affected by baseflow and snowmelt runoff.

The SWAT model achieved R² and NSE values above 0.60 during both the calibration and validation periods (Table 4, Equations 22, 23), indicating that the simulation accuracy is within a reliable range and the model performs well (Figures 5, 6). Through the calibration of sensitive parameters, the SWAT model demonstrates good applicability in the Huangyang River, making it suitable for subsequent analyses. The results show that the monthly runoff simulations align well with the observed values in most periods and vary with changes in precipitation patterns. However, there is a persistent issue with poor peak simulation results during both the calibration and validation periods. The Huangyang River is located in a mountainous area with significant variations in terrain, geology, and elevation. Although

there are many rainfall stations in the basin, data collection is difficult, leading to poor representativeness of the selected rainfall stations and weak response to localized heavy rainfall.

# 3.3 The response of runoff changes to land use changes

### 3.3.1 Analysis of land use change characteristics

Analysis of land use data for the Huangyang River Basin (Table 5 and Figure 7) based on the actual conditions of the study area and the

TABLE 4 Sensitivity analysis.

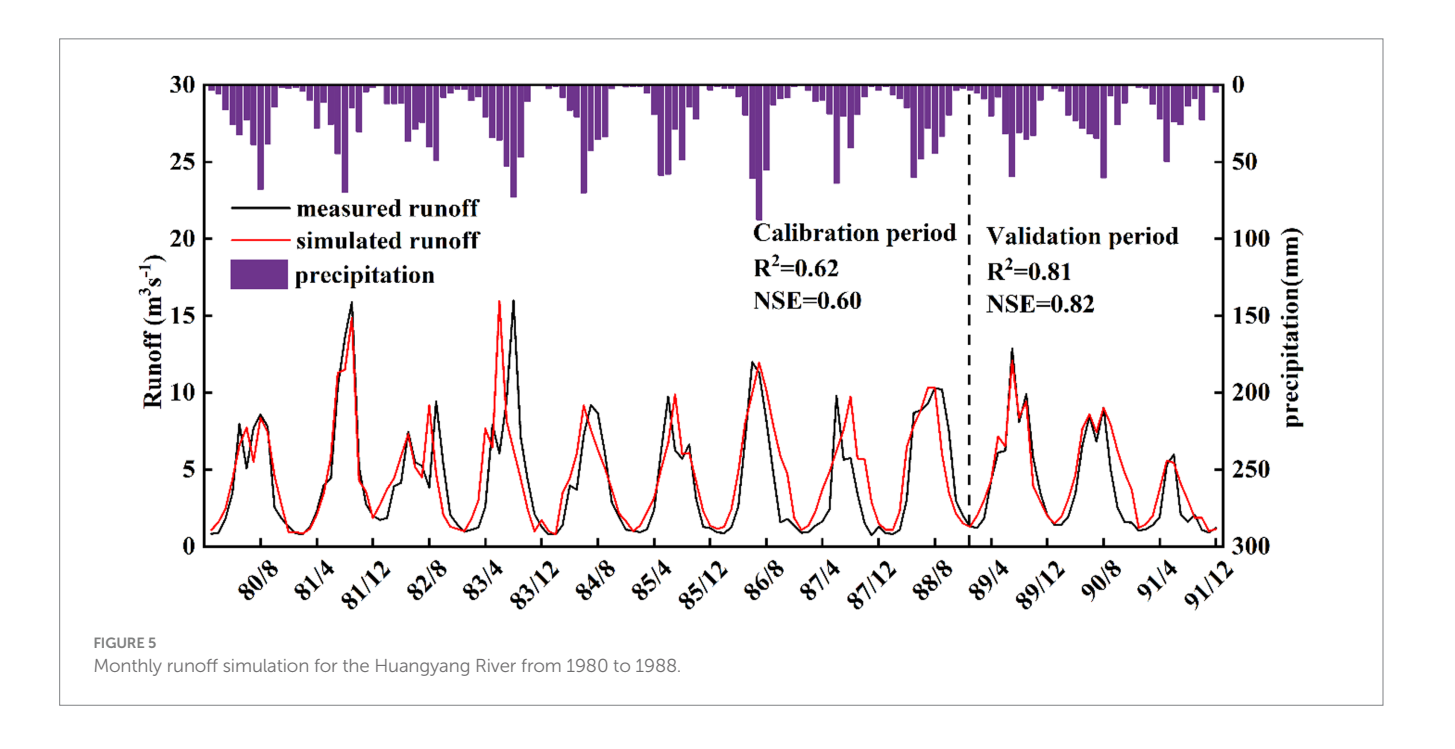
Ranking	Selected parameters	File	Range	р
1	CH_K2	rte	-0.01, 500	0.09
2	ALPHA_BF	gw	0, 1	0.09
3	SMTMP	bsn	-20, 20	0.09
4	CH_N2	rte	-0.01, 0.3	0.09
5	SFTMP	bsn	-20, 20	0.09
6	REVAPMN	gw	0, 500	0.09
7	GW_REVAP	gw	0.02, 0.2	0.13
8	SMFMN	bsn	0, 20	0.14
9	GW_DELAY	gw	0, 500	0.14
10	PLAPS	rte	-2.21	0.16
11	SMFMX	bsn	0, 20	0.25
12	GWQMN	gw	0, 5,000	0.33
13	CN2	mgt	-0.5, 0.5	0.73
14	TLAPS	sub	-10, 10	0.76
15	ESCO	hru	0, 1	0.87

land use classification in the dataset, the main land use types from 1980 to 2020 were cultivated land, forest land, grassland, unused land, water bodies, and built-up areas. Among these, grassland, forest land, and cultivated land were the dominant types, accounting for 37.33, 27.23, and 25.84% of the basin area, respectively. During the period from 1980 to 2020, forest land showed a significant increase, with the area growing from 230.42 km² in 1980 to 231.18 km² in 2020 (Equation 15). The area of cultivated land decreased from 220.27 km² in 1980 to 219.35 km² in 2020. There was no change in water bodies, a decreasing trend in unused land, and an increasing trend in built-up areas (Tables 6–10). The changes were not significant, and the magnitude of land use change, from largest to smallest, was as follows: cultivated land, grassland, built-up areas, forest land, water bodies, and unused land. The increase in forest land has ensured the security of the ecological environment.

### 3.3.2 Land use sensitivity analysis of runoff

Calculate the runoff sensitivity coefficients for different land use types during 1980–2000, 2000–2020, and 1980–2020 (Table 11, Equation 16). In the runoff sensitivity calculation, only the sensitivity of cultivated land and construction land is less than 1. Due to the small change in area, the response of cultivated land and construction land to runoff is relatively low. At the same time, the changes in forest land, grassland, and water bodies are relatively large, but their sensitivity is greater than 1, indicating a higher response of land use to runoff.

During the period of 1980–1990, the sensitivity of all land use types to runoff at the Huangyang River Reservoir Station was 0. The sensitivity of forest land was 9.35 during 2010–2020, and the sensitivity of grassland was 10.64 during 1990–2000. The sensitivity of water bodies was highest at 5.68 throughout the entire period. Due to the negligible change in unused land area, the sensitivity of unused land was 2.34 during 2010–2020, while it approached 0 in other periods. According to the stage analysis, the runoff sensitivity was significantly highest during 1990–2000 and 2010–2020, meaning that after 2000, the disturbance to the land system was relatively large, and the degree



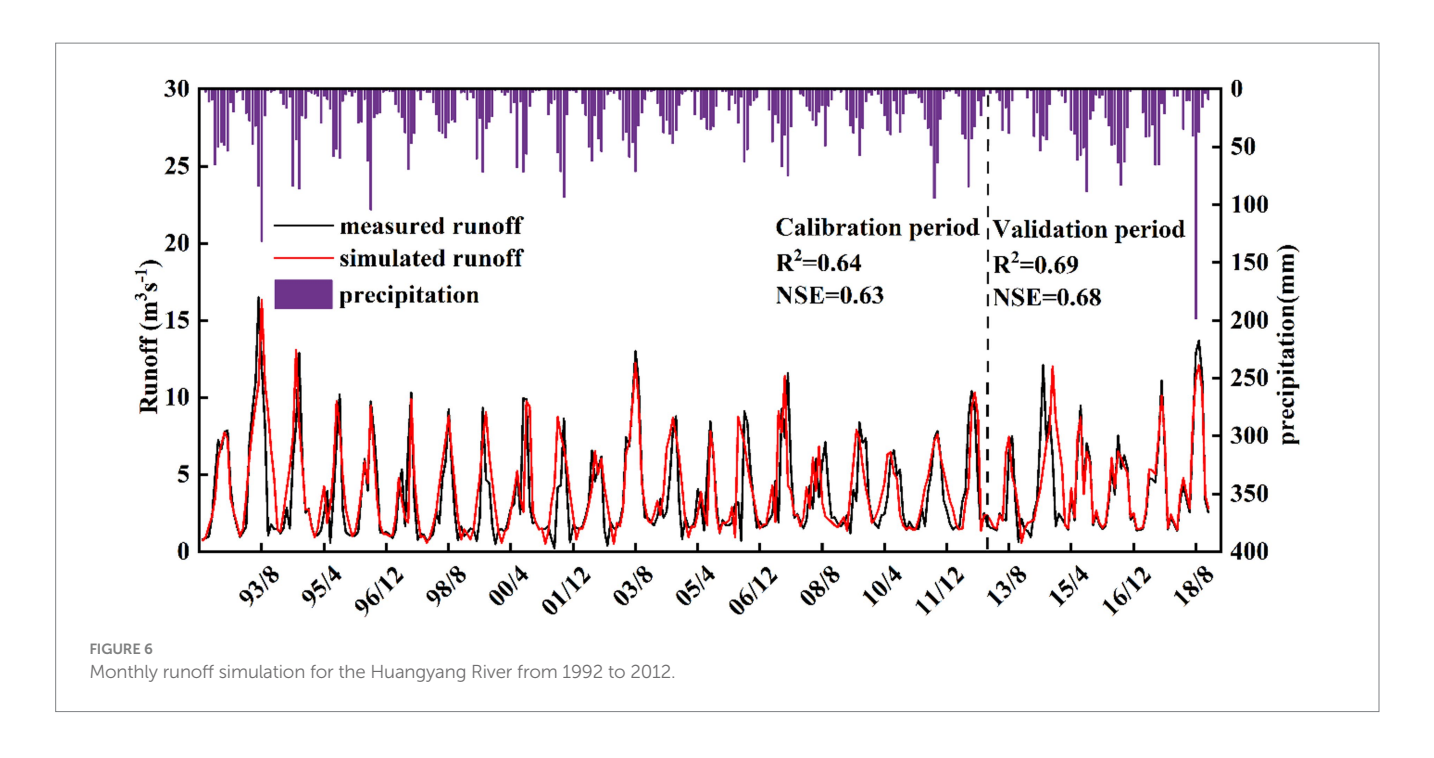


TABLE 5 Land use area of the Huangyang River from 1980 to 2020.

Land	Land use type area and rate												
use type	1980		19	990	0 2000 2010		20	2020					
	Area/ km²	Rate/%	Area/k²	Rate/%	Area/k²	Rate/%	Area/k²	Rate/%	Area/k²	Rate/%			
AGRL	220.27	25.95%	220.65	25.99%	220.34	25.96%	217.91	25.67%	219.35	25.84%			
FRST	230.42	27.14%	230.42	27.14%	230.42	27.14%	231.17	27.23%	231.18	27.23%			
PAST	316.22	37.25%	315.77	37.20%	315.78	37.20%	318.52	37.52%	316.88	37.33%			
WATR	11.79	1.39%	11.79	1.39%	11.79	1.39%	11.63	1.37%	11.77	1.39%			
URBN	6.83	0.81%	6.83	0.81%	7.14	0.84%	6.97	0.82%	7.06	0.83%			
BARR	63.36	7.46%	63.43	7.47%	63.43	7.47%	62.69	7.38%	62.65	7.38%			

of land use type transitions was higher. Therefore, the response of land use types to runoff was greatest after 2000 (Figure 8).

### 3.4 Runoff change attribution analysis

### 3.4.1 Budyko hypothesis method analysis

surface parameters, precipitation, evapotranspiration, and surface parameters (Table 12) were calculated by using Equations 1-7. Compared to the baseline period, the potential evapotranspiration at the Huangyanghe Reservoir station increased by 84.14 mm, precipitation increased by 8.53 mm, and the runoff depth decreased by 22.16 mm, while the surface characteristic parameters increased by 0.10. Thus, the runoff variation in the is negatively correlated with evapotranspiration and surface parameters. As precipitation increases, runoff also increases; when the n-value increases, runoff decreases. Compared to the baseline period, the εP increased from 0.59 to 0.64 during the change period, indicating that a 10% decrease in precipitation will reduce the runoff depth by 5.9% in the baseline period, and by 6.4% in the change period. εΕΤ0 decreased from -0.64 to -0.66, and  $\epsilon$ n decreased from -1.33 to -1.42, indicating that during the affected period, a 10.0% increase in ET0 and n will result in a 6.4 and 6.6% reduction in runoff depth, respectively. The study quantified the changes in precipitation, potential evapotranspiration, and surface parameter n, with the results showing that the largest reduction in runoff is caused by surface parameters, followed by potential evapotranspiration and precipitation. Potential evapotranspiration is the main factor driving climate change.

The contribution rates were calculated using Equations 8–14 based on the Budyko Hypothesis method. Precipitation caused a decrease of 2.74 mm in runoff, potential evapotranspiration caused a decrease of 11.28 mm in runoff, and surface parameters caused a decrease of 30.98 mm in runoff. The calculated contribution rates of precipitation, potential evapotranspiration, and surface parameters to runoff changes in the Huangyanghe were 6.10, 25.06, and 68.84%, respectively.

## 3.4.2 The attribution analysis results of the SWAT model

Based on the M-K mutation test and the sliding T-test method, 1991 was identified as the year of runoff change. The model was

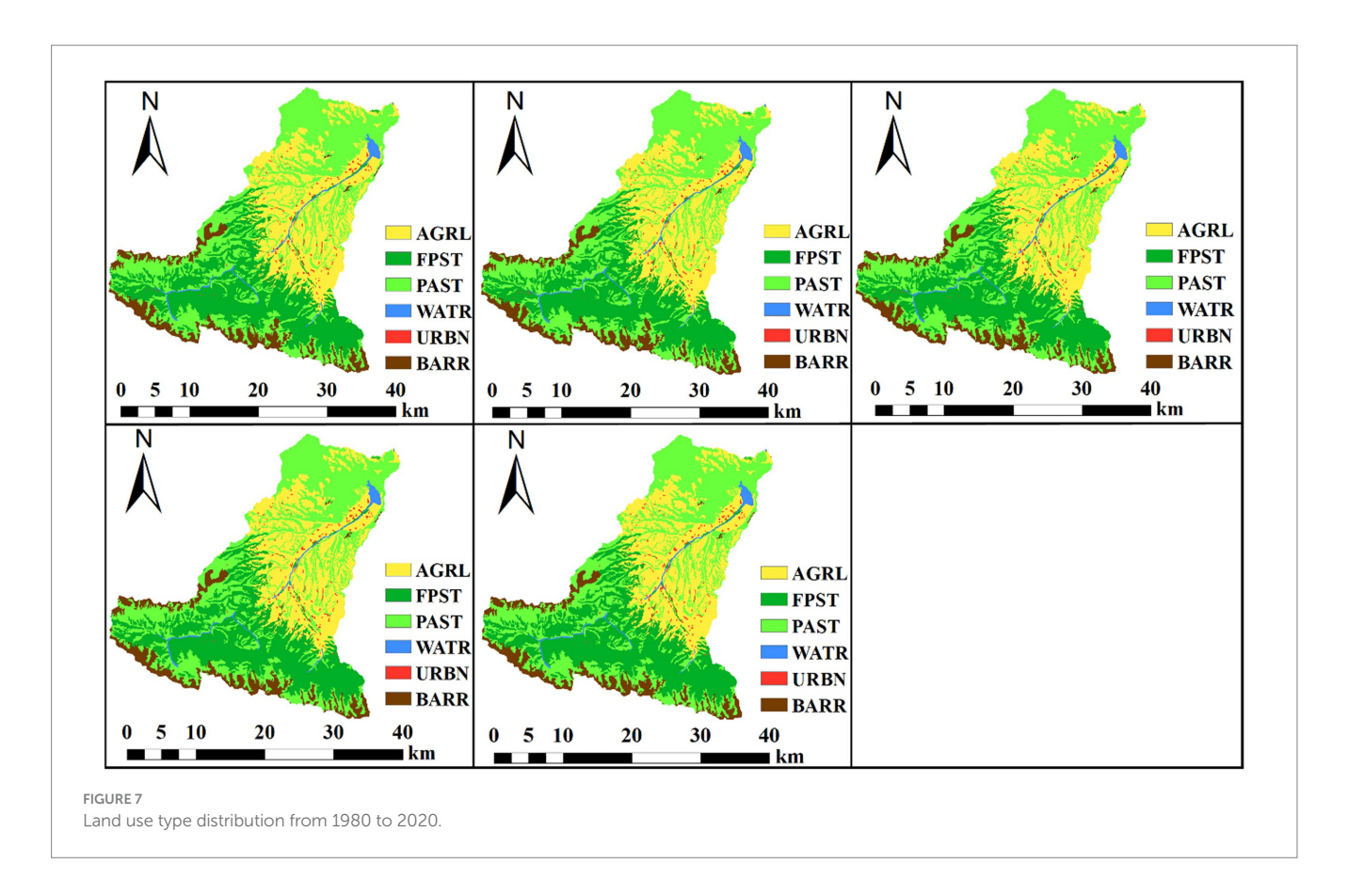


TABLE 6 Land use transformation matrix of the Huangyang River Basin from 1980 to 1990.

Year	Land use type	AGRL	FAST	PAST	WATR	URBN	BARR	Total
	AGRL	220.25	0.01	0.01	0.00	0.00		220.27
	FAST	0.01	230.41	0.00	0.00			230.42
	PAST	0.40	0.00	315.50	0.00		0.32	316.22
1980-1990	WATR	0.00	0.00		11.78			11.79
	URBN	0.00	0.00			6.83		6.83
	BARR			0.25			63.11	63.36
	Total	220.65	230.42	315.77	11.79	6.83	63.43	848.90

TABLE 7 Land use transformation matrix of the Huangyang River Basin from 1990 to 2000.

Year	Land use type	AGRL	FAST	PAST	WATR	URBN	BARR	Total
	AGRL	220.31	0.01	0.02	0.00	0.31		220.65
	FAST	0.01	230.40	0.01	0.00			230.42
	PAST	0.02	0.01	315.74			0.00	315.77
1990-2000	WATR	0.00	0.00	0.00	11.78			11.79
	URBN	0.00				6.83		6.83
	BARR			0.00			63.43	63.43
	Total	220.34	230.42	315.78	11.79	7.14	63.43	848.90

calibrated using monthly runoff data for the baseline period and the change period. The baseline period used data from 1989 to 1991 for validation, while the change period used data from 2013 to 2018 for validation. The SWAT model simulated runoff in the Huangyang River Basin, and the trend of simulated runoff was consistent with the observed runoff. Meanwhile, on the premise

TABLE 8 Land use transformation matrix of the Huangyang River Basin from 2000 to 2010.

Year	Land use type	AGRL	FAST	PAST	WATR	URBN	BARR	Total
	AGRL	215.89	0.21	4.10	0.03	0.10		220.34
	FAST	0.34	227.84	2.17	0.04	0.01	0.01	230.42
	PAST	1.39	1.87	311.85	0.03	0.01	0.62	315.78
2000-2010	WATR	0.18	0.05	0.04	11.52	0.00		11.79
	URBN	0.11	0.17	0.02		6.84		7.14
	BARR	0.00	1.04	0.33			62.05	63.43
	Total	217.91	231.17	318.52	11.63	6.97	62.69	848.90

TABLE 9 Land use transformation matrix of the Huangyang River Basin from 2010 to 2020.

Year	Land use type	AGRL	FAST	PAST	WATR	URBN	BARR	Total
	AGRL	214.70	0.45	2.12	0.25	0.38	0.00	217.91
	FAST	0.53	228.92	1.57	0.11	0.01	0.03	231.17
	PAST	3.70	1.59	312.38	0.11	0.04	0.70	318.52
2010-2020	WATR	0.12	0.16	0.06	11.29	0.01		11.63
	URBN	0.30	0.03	0.03		6.62		6.97
	BARR	0.01	0.04	0.73			61.92	62.69
	Total	219.35	231.18	316.88	11.77	7.06	62.65	848.90

TABLE 10 Land use transformation matrix of the Huangyang River Basin from 1980 to 2020.

Year	Land use type	AGRL	FAST	PAST	WATR	URBN	BARR	Total
	AGRL	214.55	0.58	4.24	0.13	0.77	0.00	220.27
	FAST	0.79	225.95	3.47	0.14	0.02	0.04	230.42
	PAST	3.48	3.32	308.02	0.14	0.04	1.22	316.22
1980-2020	WATR	0.14	0.18	0.08	11.37	0.01		11.79
	URBN	0.37	0.20	0.05		6.22		6.83
	BARR	0.01	0.94	1.02			61.39	63.36
	Total	219.35	231.18	316.88	11.77	7.06	62.65	848.90

TABLE 11 Land use sensitivity calculation.

Study period	1980–1990	1990–2000	2000–2010	2010-2020	1980-2020
AGRL	0	0.34	0.04	0.06	0.12
FAST	0	0.00	0.12 9.35		0.15
PAST	0	10.61	0.03	0.06	0.17
WATR	0	0.00	0.58	0.67	5.68
URBN	0	0.34	0.55	1.04	0.49
BARR	0	0.00	0.13	2.34	0.16

of ensuring the unchanged meteorological data during the change period, the land use data is replaced to conduct SWAT runoff simulation. Both NSE and R<sup>2</sup> were above 0.60, indicating that the simulation results are highly reliable. The contribution rates of climate change and human activities to runoff were calculated using Equations 17–21. The contribution rate of climate change

in the Huangyang River Basin is 30.48%, while that of human activities is 69.52%. Among them, the contribution rate of land use change is 10.70%, and that of other human activities is 58.82% (Table 13).

The SWAT model simulation results were compared with the estimates from the Budyko hypothesis method (Table 14). Both

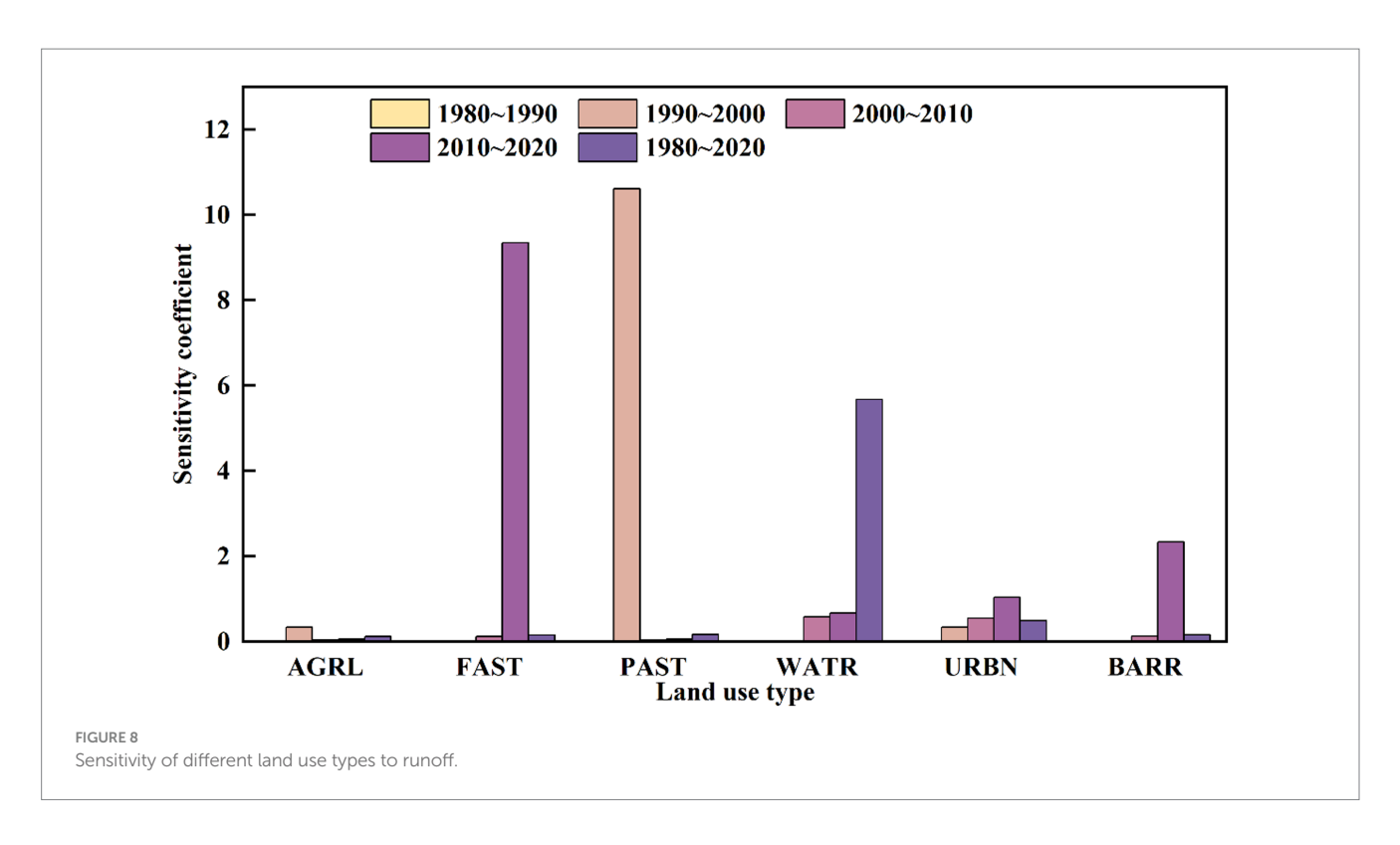


TABLE 12 Sensitivity coefficients of various influencing factors.

Station	Period	PET/mm	R/mm	P/mm	n	R/P	PET/P	Elas	Elastic coefficient	
								$arepsilon_p$	$arepsilon_{ET_{_{0}}}$	$\varepsilon_n$
Huangyang	1957-1991	603.04	161.79	269.34	0.54	0.60	2.24	0.59	-0.64	-1.33
River	1992-2023	687.14	139.63	277.87	0.64	0.50	2.47	0.64	-0.66	-1.42

methods identified the same driving factors for runoff changes, with human activities being the key factor in runoff reduction. However, there is a discrepancy in the relative contribution rates between the SWAT model and the Budyko hypothesis method. The Budyko simulation results showed a climate change contribution rate of 31.16% and a human activity contribution rate of 68.84%. In the estimation, climate change considered factors such as precipitation and potential evapotranspiration, while human activities were reflected by the parameter "n," which includes land use changes and other underlying surface factors. Most current studies overlook changes in water storage (such as water withdrawal, irrigation, and hydraulic engineering), leading to the parameter "n" being mostly attributed to land use changes. Some studies have shown that changes in water storage cause greater runoff variation than precipitation (Ohta et al., 2008), meaning the Budyko hypothesis method may underestimate the contribution of human activities to runoff. The SWAT model simulated a climate change contribution rate of 30.48% and a human activity contribution rate of 69.52%, the contribution rate of human activities is higher than the Budyko hypothesis method's estimates. This finding is consistent with the research results of Wu et al. (2017) and Xu et al. (2023). The SWAT model, by comprehensively considering the effects of meteorology, soil, land use, and slope on hydrological processes, has been proven to be a more accurate attribution analysis tool, even though meteorological, land use, and

soil type data limitations may prevent the full manifestation of human activities in the modeling process.

### 4 Discussion

# 4.1 The driving mechanisms of runoff changes

### 4.1.1 The impact of climate change on runoff

In the arid northwest region, climate change (such as P and PET) is a key factor affecting water resources, among which precipitation is usually regarded as the main natural driver of runoff variation (Berghuijs et al., 2017). The annual precipitation in the Huangyang River Basin shows an insignificant increasing trend (the annual linear trend rate is 0.13 mm/a, Figure 9). The results of the attribution analysis indicated that the change in P was not the main driving factor for the observed reduction in runoff during the study period. Meanwhile, PET shows a significant increasing trend (with an annual linear trend rate of 0.28 mm/a), which is consistent with the observed rising trend of surface temperature. Theoretically, the increase of PET, especially in arid areas with limited water resources, may intensify actual evapotranspiration, resulting in more water loss through evaporation (Carter and Liang, 2019; Hoek van Dijke et al., 2022). Based on the facts that precipitation

Other human activities 58.82 decrement Ξ Human activities Rate% land use change decrement Climate change 5.7 18.7 Simulated runoff (mm) 149 151 runoff (mm Observed 178.7 09 1992-2023 1956-1991 Period

IABLE 13 Attribution analysis of runoff change using the SWAT model.

changes are weak and insignificant, PET increases significantly, and runoff decreases significantly, the analysis results indicate that the relative contribution of PET changes to the reduction of runoff during the study period may be more significant than that of precipitation changes.

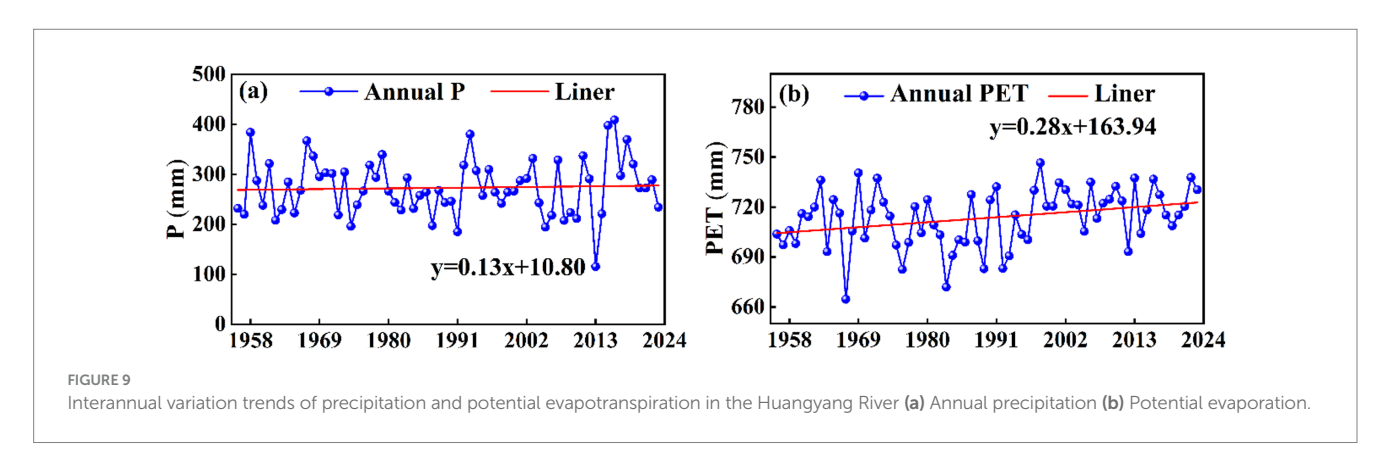
In addition, before and after the sudden change of the Huangyang River runoff, there was a significant correlation among P, PET and the runoff volume (Figure 10). This confirms the fundamental hydrological law that P remains the fundamental source of runoff replenishment in this basin. However, a key phenomenon is that although precipitation showed a weak increasing trend during the study period, runoff decreased significantly. This phenomenon of "increased precipitation and decreased runoff" contradicts the scenario dominated solely by climate fluctuations (such as reduced P or increased PET), strongly suggesting that other factors (mainly human activities) have significantly interferes with the hydrological processes in the basin, weakening or even reversing the possible runoff replenishment effect brought about by increased precipitation. Therefore, the comprehensive attribution analysis results (including climate resilience methods, hydrological model simulations, etc.) indicate that human activities are the dominant factor for the reduction of runoff in the Huangyang River Basin during the study period. This understanding is consistent with the research conclusions of Xue (2021) and Chen (2023) in this region.

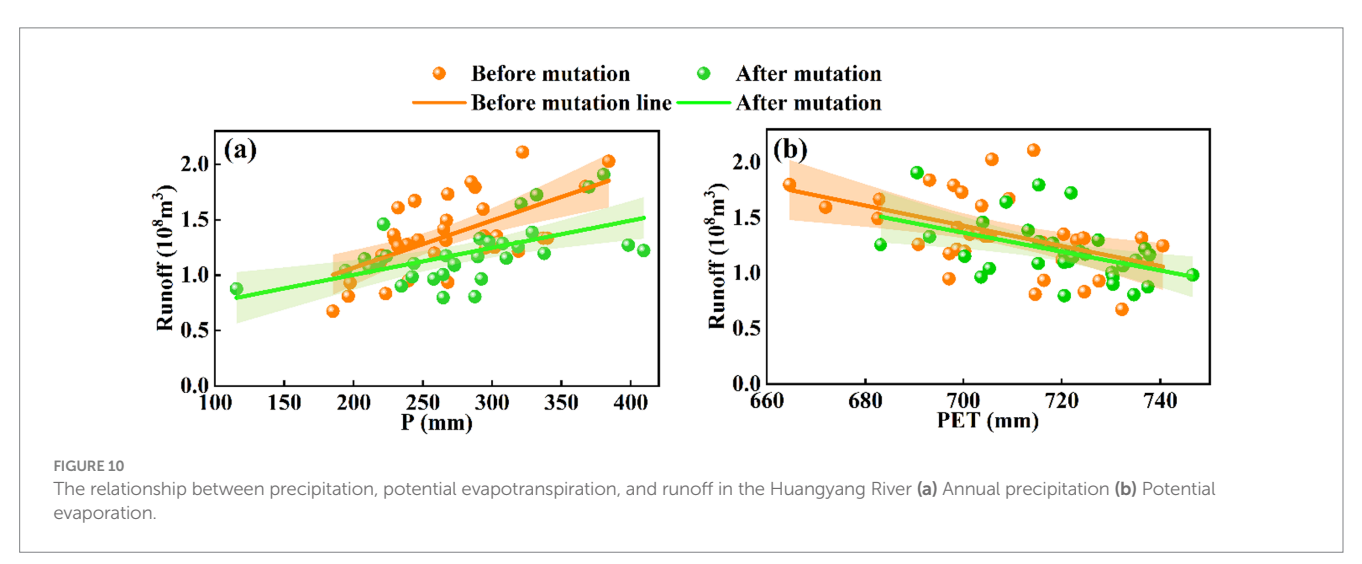
### 4.1.2 The impact of human activities on runoff

Apart from climate change, human activities are also important factors causing changes in runoff. Human activities that lead to a decrease in runoff include land use/vegetation cover changes, industrial and agricultural water usage, and water conservancy projects (Zhai and Tao, 2017). Since 1956, driven by human activities such as reservoir construction, ecological governance and water-saving measures, the runoff process and water resources pattern in the Huangyang River Basin have undergone significant changes. While the Huangyang River Reservoir (1960) enhanced irrigation security, it led to a reduction of approximately 5% in upstream runoff and discretized the annual runoff sequence (Luo et al., 2024). Since 2000, the policy of returning farmland to forest has enhanced the stability of base flows, leading to a rise in groundwater levels. The dry season runoff has increased by 15%, but the flood peak during the flood season has been reduced by 39% (Hu et al., 2025). After 2010, efficient water-saving and ecological water conveyance projects were implemented. To ensure that the water flow at the sections met the standards, the policies for the Huangyang River were significantly adjusted. Overall, human activities have become the dominant factor driving the spatio-temporal evolution of runoff in the Huangyang River Basin. From 1980 to 2020, the cultivated land area in the Huangyang River Basin continued to shrink, while the grassland and forest land areas increased significantly. The analysis of land use transformation shows that cultivated land is mainly converted into grassland and forest land, reducing the damage to natural vegetation and facilitating ecological restoration. However, the evapotranspiration of grassland is relatively high, and the grassroots layer is prone to form a dense and weakly permeable structure, which limits soil water infiltration and base flow replenishment (Zhang et al., 2001; Shao et al., 2023); Forest land consumes a large amount of soil moisture through deep root

TABLE 14 Contribution rates of climate change and human activities to runoff variations based on the Budyko hypothesis method.

Station	$\Delta R_P$	$\Delta R_{PET}$	$\Delta R_n$	$\Delta R$	$\Delta R'$	$C_P/\%$	C <sub>PET</sub> /%	<i>C<sub>n</sub></i> /%
Huangyang River	-2.74	-11.28	-30.98	-16.55	-45.00	6.10	25.06	68.84





systems, further inhibiting runoff formation (Zhao et al., 2025). Although the above process led to the reduction of runoff to a certain extent, the downward trend of runoff slowed down after 2000. This was mainly attributed to the enhanced canopy interception effect due to the increase in vegetation coverage: a large amount of precipitation was intercepted at the surface layer of vegetation, reducing direct evaporation and deep seepage, thereby maintaining the spatiotemporal stability of surface water (Bai et al., 2020; Qiu et al., 2022). Therefore, although the reduction of cultivated land and the expansion of forest and grassland generally tend to weaken runoff, under high coverage conditions, the regulation and storage effect of vegetation structure may have a certain buffering effect on the runoff process, reflecting the phased influence of different ecological mechanisms on the evolution of runoff. This change can mainly be attributed to the implementation of a series of national and local ecological projects (Gansu Province Shiyang River Basin Key Management Plan). Under policy-driven measures, the upper reaches of the Shiyang River have implemented strategies such as mountain closure for afforestation, and returning cultivated land to forests and grasslands, which significantly improved the regional vegetation cover and ecological environment. Vegetation restoration has enhanced the water conservation function in the upper reaches of the basin, manifested by: effective interception of rainfall, increased infiltration, and improved soil moisture content (Qiu et al., 2022; Wang D. et al., 2019). As a result, runoff from the upper reaches of the Shiyang River increased, partly benefiting from the success of these ecological restoration projects, indicating that moderate human activities and climate change can increase runoff. However, the decrease in runoff in the Huangyang River Basin suggests that human activities are more frequent. Therefore, for future watershed water resource management, the upper reaches of the Shiyang River should continue to strengthen natural protected area conservation, further improve forest and grass cover, and consolidate and enhance water source conservation capacity. At the same time, a "zoned water-appropriate" management strategy should be implemented. It is recommended to prioritize low-water-consuming vegetation (such as Caragana and Seabuckthorn) in low-altitude areas, while preserving natural grasslands in high-altitude areas to maintain stable base flow.

To further assess the extent of human activities' impact on the Huangyang River, this study defines the sum of the areas of construction land and cultivated land as the human activity area ratio (30.2%) and selects population density and the reservoir storage capacity coefficient (CSRC) as key analytical indicators. The basin has a high population density, coupled with a relatively high human activity area ratio, indicating significant human transformation of the underlying surface and a large consumption of water resources. Reservoirs, dams, and other projects significantly alter the water balance of the basin by impounding and regulating surface runoff, leading to a general reduction in runoff during summer and a general increase in runoff during winter (Su et al., 2025). The regulation capacity of reservoirs can be measured by the storage capacity coefficient (CSRC): CSRC > 30% indicates multi-year regulation,  $8\% \le CSRC < 30\%$  indicates annual regulation,  $3\% \le CSRC < 8\%$ indicates seasonal regulation, and CSRC < 3% indicates daily regulation (Li Z. et al., 2025). The Huangyang River reservoir is classified as annual regulation (CSRC = 24.76), indicating a strong runoff regulation ability and a strong correlation between runoff changes and reservoir regulation. In the study of watershed models, Manli found that when reservoir regulation reduced summer runoff by 10%, winter runoff increased by 8.3% compared to the previous year, confirming the dominant role of human activities (reservoirs) in seasonal water volume (Zhu et al., 2015).

### 4.2 Uncertainty and limitations

The Budyko-based elasticity approach provides a rapid means to quantify the combined impacts of climate variability and land surface changes. However, the physical interpretation of the parameter n remains inherently ambiguous. Variations in n can simultaneously represent multiple hydrological processes. For example, an increase in n may indicate enhanced evapotranspiration induced by vegetation restoration, but it may also reflect accelerated runoff generation caused by soil compaction and reduced infiltration. Wang et al. (2018) demonstrated that in the Yellow River Basin, population density accounted for 128.7% of the observed increase in n, underscoring the strong influence of human-induced land surface modifications. Similarly, higher NDVI values tend to elevate n by promoting evapotranspiration and reducing runoff, whereas urban expansion and population growth increase n while accelerating runoff through reduced infiltration. These patterns highlight the necessity of distinguishing the differential contributions of vegetation restoration and soil hardening to the evolution of n and improving the Budyko framework to alleviate its inherent parameter ambiguity (Han et al., 2023). Furthermore, uncertainties in precipitation and potential evapotranspiration (PET) measurements can directly propagate to the elasticity-based attribution results. In contrast, the SWAT model employs spatially explicit parameterization of land use and soil properties, such as curve number values and leaf area index, to represent the hydrological response to vegetation and land surface dynamics more mechanistically (Figure 7). This enables a more explicit separation of the impacts of climate variability and human activities. Nevertheless, model performance is constrained by multiple factors. The evident bias in peak flow simulations (Table 3) indicates the challenges of representing the nonlinear rainfall-runoff relationships in mountainous catchments (Wu L. et al., 2022; Zhao et al., 2025). This limitation likely reflects the combined effects of sensitivity to localized precipitation, insufficient representation of small-scale runoff generation processes, and data gaps regarding the operation of water conservancy projects. In addition, SWAT results are highly dependent on parameter calibration, and uncertainties in soil, vegetation, and climate data can further propagate through the model.

The Budyko and SWAT approaches exhibit complementary strengths and weaknesses. The Budyko framework is robust for long-term, climate-dominated hydrological assessment but may overestimate climate contributions under intensive human disturbance. SWAT, while process-based and capable of explicitly representing land use effects, is susceptible to parameterization and data uncertainties. To enhance the robustness of runoff attribution, future studies should: (i) incorporate multi-source observations (e.g., remote sensing evapotranspiration and isotopic tracers) to constrain model parameters; (ii) conduct comprehensive sensitivity and uncertainty analyses to quantify confidence intervals of attribution results; and (iii) adopt a multi-method comparative framework to reconcile potential biases and improve the reliability of hydrological inferences.

### 5 Conclusion

This study integrates multi-source remote sensing data, distributed hydrological simulation, and the Budyko water–heat coupling theory to systematically analyze the driving mechanisms of runoff changes in the Huangyang River Basin from 1956 to 2023. The main conclusions are as follows.

The annual runoff has significantly decreased at a rate of  $0.042 \times 10^8 \, \mathrm{m}^3 \cdot \mathrm{a}^{-1}$  (p < 0.05), with 1991 being the inflection point of runoff change. At the seasonal scale, a "winter increase, summer decrease" pattern is observed: winter runoff increased significantly at a rate of  $0.40 \times 10^8 \, \mathrm{m}^3/10a$ , while the trend of summer runoff reduction was alleviated after 2000 due to the implementation of ecological projects.

Human activities are the dominant factor in runoff reduction: the attribution results of the SWAT model and the Budyko hypothesis method are consistent, with human activities contributing 69.52 and 68.84%, respectively, while climate change contributes 30.48 and 31.16%. Human activities alter hydrological processes through two main pathways: land use transformation (from cropland to forest/grassland) and the annual regulation effect of reservoirs. The regulation effect of the Huangyang River Reservoir (with a storage capacity coefficient of 24.76%) significantly changes the intra-annual distribution of runoff, characterized by summer storage and winter replenishment.

The expansion of forest and grassland from 1980 to 2020 has led to an increase in evapotranspiration water consumption in the basin. Sensitivity analysis shows that water bodies (with a sensitivity of 5.68) and forests (with a sensitivity of 9.35 from 2010 to 2020) respond strongly to changes in runoff. This reveals the "water-ecology" trade-off effect of vegetation restoration: although ecological projects improve water conservation capacity, the expansion of high-water-consumption vegetation exacerbates water resource pressure, necessitating the optimization of vegetation structure and coverage.

### Data availability statement

The original contributions presented in the study are included in the article/supplementary material, further inquiries can be directed to the corresponding author.

### **Author contributions**

WL: Software, Visualization, Writing – review & editing, Writing – original draft, Resources, Conceptualization, Data curation, Validation. PC: Visualization, Resources, Writing – review & editing, Data curation, Validation, Investigation, Software. KL: Writing – review & editing, Investigation, Software, Visualization, Formal analysis, Methodology. HS: Validation, Writing – review & editing, Project administration, Supervision, Funding acquisition.

### **Funding**

The author(s) declare that financial support was received for the research and/or publication of this article. This study was partially supported by the Doctoral Foundation of Gansu Agricultural University (No. GAU-KYQD-2022-04), Gansu Provincial Water Science Experimental Research and Technology Extension Project (Nos. 25GSLK103 and 25GSLK087).

### References

Abbaspour, K. C., Rouholahnejad, E., Vaghefi, S. R. I. N. I. V. A. S. A. N. B., Srinivasan, R., Yang, H., and Klove, B. (2015). A continental-scale hydrology and water quality model for Europe: calibration and uncertainty of a high-resolution large-scale SWAT model. *J. Hydrol.* 524, 733–752. doi: 10.1016/j.jhydrol.2015.03.027

Arnold, J. G., Srinivasan, R., Muttiah, R. S., and Williams, J. R. (1998). Large area hydrologic modeling and assessment part I: model development 1. *JAWRA J. Am. Water Resour. Assoc.* 34, 73–89. doi: 10.1111/j.1752-1688.1998.tb05961.x

Bai, P., Liu, X., Zhang, Y., and Liu, C. (2020). Assessing the impacts of vegetation greenness change on evapotranspiration and water yield in China. *Water Resour. Res.* 56:e2019WR027019. doi: 10.1029/2019WR027019

Berghuijs, W. R., Larsen, J. R., van Emmerik, T. H., and Woods, R. A. (2017). A global assessment of runoff sensitivity to changes in precipitation, potential evaporation, and other factors. *Water Resour. Res.* 53, 8475–8486. doi: 10.1002/2017WR021593

Carter, C., and Liang, S. (2019). Evaluation of ten machine learning methods for estimating terrestrial evapotranspiration from remote sensing. *Int. J. Appl. Earth Obs. Geoinf.* 78, 86–92. doi: 10.1016/j.jag.2019.01.020

Chen, J. X., Xia, J., Zhao, C. S., Zhang, S. F., Fu, G. B., and Ning, L. K. (2014). The mechanism and scenarios of how mean annual runoff varies with climate change in Asian monsoon areas. *J. Hydrol.* 517, 595–606. doi: 10.1016/j.jhydrol.2014.05.075

Chen, Z. X. (2023). Simulation and projection of mountainous runoff in the Shiyang River basin under climate change. (Master's thesis). Lanzhou: Lanzhou Jiaotong University.

Choudhury, B. (1999). Evaluation of an empirical equation for annual evaporation using field observations and results from a biophysical mode. *J. Hydrol.* 216, 99–110.

Duan, R. (2023). Quantitative analysis of the effects of climate change and human activities on the runoff in the Shiyang River basin. (Master's thesis). Lanzhou: Lanzhou University of Technology (In Chinese).

Feng, L., Chen, Y., Guo, M., Wang, W., Lou, Y., Chen, Z., et al. (2025). Effect of dominant vegetation under long-term natural and artificial vegetation restoration modes on gully slope stability considering rainfall and topography interactions. *Catena*. 256:109067. doi: 10.1016/j.catena.2025.109067

Han, P. F., Sankarasubramanian, A., Wang, X. S., Wan, L., and Yao, L. O. (2023). Parameter analytical derivation in modified Budyko framework for unsteady - state

### Conflict of interest

The authors declare that the research was conducted in the absence of any commercial or financial relationships that could be construed as a potential conflict of interest.

### Generative AI statement

The authors declare that no Gen AI was used in the creation of this manuscript.

Any alternative text (alt text) provided alongside figures in this article has been generated by Frontiers with the support of artificial intelligence and reasonable efforts have been made to ensure accuracy, including review by the authors wherever possible. If you identify any issues, please contact us.

### Publisher's note

All claims expressed in this article are solely those of the authors and do not necessarily represent those of their affiliated organizations, or those of the publisher, the editors and the reviewers. Any product that may be evaluated in this article, or claim that may be made by its manufacturer, is not guaranteed or endorsed by the publisher.

streamflow elasticity in humid catchments. Water Resour. Res. 59:e2023WR034725. doi: 10.1029/2023WR034725

He, Y., Jiang, X., Wang, N., Zhang, S., Ning, T., Zhao, Y., et al. (2019). Changes in mountainous runoff in three inland river basins in the arid Hexi corridor, China, and its influencing factors. *Sustain. Cities Soc.* 50:101703. doi: 10.1016/j.scs.2019.101703

He, Y., Wang, F., Mu, X. M., Guo, L. Q., Gao, P., and Zhao, G. J. (2017). Human activity and climate variability impacts on sediment discharge and runoff in the Yellow River of China. *Theor. Appl. Climatol.* 129, 645–654. doi: 10.1007/s00704-016-1796-8

Hoek van Dijke, A. J., Herold, M., Mallick, K., Benedict, I., Machwitz, M., Schlerf, M., et al. (2022). Shifts in regional water availability due to global tree restoration. *Nat. Geosci.* 15, 363–368. doi: 10.1038/s41561-022-00935-0

Hu, J., Ma, J., Nie, C., Xue, L., Zhang, Y., Ni, F., et al. (2020). Attribution analysis of runoff change in Mintuo River basin based on SWAT model simulations, China. *Sci. Rep.* 10:2900. doi: 10.1038/s41598-020-59659-z

Hu, T. M., Wang, Z. L., and Zhang, L. (2025). Shiyang river basin runoff evolution characteristics and its driving mechanism study. *J. Yellow River Water Conserv. Vocat. Techn. College.* 1–7. (In Chinese)

Hu, Y., Duan, W., Chen, Y., Zou, S., Kayumba, P. M., and Sahu, N. (2021). An integrated assessment of runoff dynamics in the Amu Darya River basin: confronting climate change and multiple human activities, 1960–2017. *J. Hydrol.* 603:126905. doi: 10.1016/j.jhydrol.2021.126905

Jiang, K., Mo, S., Yu, K., Li, P., and Li, Z. (2024). Analysis on the relationship between runoff erosion power and sediment transport in the Fujiang River basin and its response to land use change. *Ecol. Indic.* 159:111690. doi: 10.1016/j.ecolind.2024.111690

Jun, Z. J., Ming, L. K., Qiang, C. Y., Min, W., and Xin, P. Z. (2022). Impacts of changing conditions on the ecological environment of the Shiyang River basin, China. *Water Supply* 22, 5689–5697. doi: 10.2166/ws.2022.197

Kim, D., and Chun, J. A. (2021). Revisiting a two-parameter Budyko equation with the complementary evaporation principle for proper consideration of surface energy balance. *Water Resour. Res.* 57:57. doi: 10.1029/2021WR030838

Lan, Z., Zhao, Y., Zhang, J., Jiao, R., Khan, M. N., Sial, T. A., et al. (2021). Long-term vegetation restoration increases deep soil carbon storage in the Northern Loess Plateau. *Sci. Rep.* 11:13758. doi: 10.1038/s41598-021-93157-0

Li, L., Long, D., Wang, Y., and Woolway, R. I. (2025). Global dominance of seasonality in shaping lake-surface-extent dynamics.  $Nature\,642,361-368.$  doi:10.1038/s41586-025-09046-3

- Liu, C. X., Chen, Y. N., Fang, G. H., Zhou, H. H., Huang, W. J., Liu, Y. C., et al. (2022). Hydrological connectivity improves the water-related environment in a typical arid Inland River basin in Xinjiang, China. *Remote Sens* 14:14. doi: 10.3390/rs14194977
- Liu, J., Liu, M., Tian, H., Zhuang, D., and Deng, X. (2005). Spatial and temporal patterns of China's cropland during 1990 ~ 2000: an analysis based on Landsat tm data. *Remote Sens. Environ.* 98, 442–456. doi: 10.1016/j.rse.2005.08.012
- Liu, J., Zhang, Q., and Sun, H. (2021). SWAT-based simulation of oasis water balance under land use change in the Huangyang River basin. *Arid Land Geogr.* 44, 1351–1359.
- Liu, W. L., Hua, H. L., Zhang, J. R., Wang, J., Wang, Y. F., and Liu, L. N. (2022). Attribution identification of runoff variation in Ganjiang River basin based on Budyko hypothesis. *Pearl River* 43, 90–97. (In Chinese)
- Li, Z., Liu, F., Li, H., Liu, M., Li, Z., Feng, Q., et al. (2025). Driving forces of the spatiotemporal supply pattern of runoff in the source region of Yellow River. *J. Hydrol. Reg. Stud.* 60:102515. doi: 10.1016/j.ejrh.2025.102515
- Li, Z. S., Li, Y. G., Feng, Q., Zhu, M., Lv, Y. M., Gui, J., et al. (2017). The contribution and influence of cryospheric meltwater in the Shiyang River basin on outflow runoff. *Quat. Res.* 37, 1045–1054. (In Chinese)
- Luo, Y., Lu, Z. X., Feng, Q., Zhu, M., and Zhang, J. B. (2024). The changes in the annual distribution of mountain runoff during the period of 1965-2018 in Hexi corridor, Northwest China. *Res. Cold Arid Reg.* 16, 73–83. doi: 10.1016/j.rcar.2024.04.001
- Nalley, D., Adamowski, J., Biswas, A., Gharabaghi, B., and Hu, W. (2019). A multiscale and multivariate analysis of precipitation and streamflow variability in relation to ENSO, NAO and PDO. *J. Hydrol.* 574, 288–307. doi: 10.1016/j.jhydrol.2019.04.024
- Ohta, T., Maximov, T. C., Dolman, A. J., Nakai, T., van der Molen, M. K., Kononov, A. V., et al. (2008). Interannual variation of water balance and summer evapotranspiration in an eastern Siberian larch forest over a 7-year period (1998-2006). *Agric. For. Meteorol.* 148, 1941–1953. doi: 10.1016/j.agrformet.2008.04.012
- Praveen, B., Talukdar, S., Shahfahad, Mahato, S., Mondal, J., Sharma, P., et al. (2020). Analyzing trend and forecasting of rainfall changes in India using non-parametrical and machine learning approaches. *Sci. Rep.* 10:10342. doi: 10.1038/s41598-020-67228-7
- Qiu, D., Xu, R., Wu, C., Mu, X., Zhao, G., and Gao, P. (2022). Vegetation restoration improves soil hydrological properties by regulating soil physicochemical properties in the loess plateau, China. *J. Hydrol.* 609:127730. doi: 10.1016/j.jhydrol.2022.127730
- Raffar, N., Zulkafli, Z., Yiwen, M., Muharam, F. M., Rehan, B. M., and Nurulhuda, K. (2022). Watershed-scale modelling of the irrigated rice farming system at Muda, Malaysia, using the soil water assessment tool. *Hydrol. Sci. J.* 67, 462–476. doi: 10.1080/02626667.2021.2022682
- Raihan, F., Beaumont, L. J., Maina, J., Saiful Islam, A., and Harrison, S. P. (2020). Simulating streamflow in the upper Halda Basin of southeastern Bangladesh using SWAT model. *Hydrol. Sci. J.* 65, 138–151. doi: 10.1080/02626667.2019.1682149
- Shao, Y., Dong, Z., Meng, J., Wu, S., Li, Y., Zhu, S., et al. (2023). Analysis of runoff variation and future trends in a changing environment: case study for Shiyanghe River basin, Northwest China. *Sustainability* 15:2173. doi: 10.3390/su15032173
- Si, W. A., Huang, Y., Liu, T., Li, Z. X., Zan, C. J., and Wang, X. F. (2025). Application of deep learning and temperature spatial field in the runoff simulation of headwaters of the Yarkant River. *Prog. Geogr.* 44, 631–641. (In Chinese)
- Su, X., Bejarano, M. D., Jansson, R., Pilotto, F., Sarneel, J. M., Lin, F., et al. (2025). Broad scale meta-analysis of drivers mediating adverse impacts of flow regulation on riparian vegetation. *Glob. Chang. Biol.* 31:e70042. doi: 10.1111/gcb.70042
- Wang, D., Yu, X., Jia, G., and Wang, H. (2019). Sensitivity analysis of runoff to climate variability and land-use changes in the Haihe Basin mountainous area of North China. *Agric. Ecosyst. Environ.* 269, 193–203. doi: 10.1016/j.agee.2018.09.025
- Wang, L., Liu, T. T., and Xie, J. Z. (2019). Research on the impact of land use scenario changes on runoff in the qingshui river basin of zhangjiakou based on SWAT model. Soil

- *Water Conserv. Res.* 26, 245–251. doi: 10.13869/j.carolcarrollnkiRSWC.2019.04.037. (In Chinese)
- Wang, M., Zhang, S., Guo, X., Xiao, L., Yang, Y., Luo, Y., et al. (2024). Responses of soil organic carbon to climate extremes under warming across global biomes. *Nat. Clim. Chang.* 14, 98–105. doi: 10.1038/s41558-023-01874-3
- Wang, Q., Guan, Q., Sun, Y., Du, Q., Xiao, X., Luo, H., et al. (2023). Simulation of future land use/cover change (LUCC) in typical watersheds of arid regions under multiple scenarios. *J. Environ. Manag.* 335:117543. doi: 10.1016/j.jenvman.11754
- Wang, W., Lu, W., Xing, W., Li, J., and Li, C. (2018). Analysis of change and attribution of Budyko equation parameter n in Yellow River. *Water Resour. Prot.* 34, 7–13. doi: 10.2139/ssrn.5109500
- Wu, J., Miao, C., Zhang, X., Yang, T., and Duan, Q. (2017). Detecting the quantitative hydrological response to changes in climate and human activities. *Sci. Total Environ.* 586, 328–337. doi: 10.1016/j.scitotenv.2017.02.010
- Wu, L., Liu, X., Yang, Z., Yu, Y., and Ma, X. (2022). Effects of single-and multi-site calibration strategies on hydrological model performance and parameter sensitivity of large scale semi -arid and semi humid watersheds. *Hydrol. Process.* 36:e14616. doi: 10.1002/hyp.14616
- Wu, Z. Q., Liu, X. C., Liu, Q., Qiao, R. L., Liu, Z. Y., Yang, T., et al. (2022). Urban development strategies in China based on water resource constraints. *Strategic Study CAE* 24, 75–88. (In Chinese). doi: 10.15302/J-SSCAE-2022.05.010
- Xue, D. X. (2021). Attribution analysis of runoff changes in the Shiyang River basin. (Master's thesis). Lanzhou: Northwest Normal University.
- Xu, R., Qiu, D., Wu, C., Mu, X., Zhao, G., Sun, W., et al. (2023). Quantifying climate and anthropogenic impacts on runoff using the SWAT model, a Budyko-based approach and empirical methods. *Hydrol. Sci. J.* 68, 1358–1371. doi: 10.1080/02626667. 2023.2218551
- Yang, H., Yang, D., Lei, Z., and Sun, F. (2008). New analytical derivation of the mean annual water-energy balance equation. *Water Resour. Res.* 44, 893–897. doi: 10.1029/2007WR006135
- Yao, J. Q., Zhao, Q. D., and Liu, Z. H. (2015). Effect of climate variability and human activities on runoff in the Jinghe river basin, Northwest China. *J. Mt. Sci.* 12, 358–367. doi: 10.1007/s11629-014-3087-0
- Yuan, Z., Yan, D., Yang, Z., Xu, J., Huo, J., Zhou, Y., et al. (2018). Attribution assessment and projection of natural runoff change in the Yellow River Basin of China. *Mitig. Adapt. Strateg. Glob. Chang.* 23, 27–49. doi: 10.1007/s11027-016-9727-7
- Zhai, R., and Tao, F. (2017). Contributions of climate change and human activities to runoff change in seven typical catchments across China. *Sci. Total Environ.* 605-606, 219–229. doi: 10.1016/j.scitotenv.2017.06.210
- Zhang, L., Dawes, W. R., and Walker, G. R. (2001). Response of mean annual evapotranspiration to vegetation changes at catchment scale. *Water Resour. Res.* 37, 701–708. doi: 10.1029/2000wr900325
- Zhao, X. Y., Zhang, X., and Sun, Y. (2023). The impact of land use change on runoff in the wuding river basin from 2005 to 2030. *People's Yellow River*. 45, 24–31. (In Chinese)
- Zhao, Y., Zhang, R., Shu, H., Li, Y., Xu, Z., and Wang, Q. (2025). Study on the driving factors of watershed runoff change in Zuli River by Budyko hypothesis and soil and water assessment tool model. *Ecol. Indic.* 170:112963. doi: 10.1016/j.ecolind. 2024.112963
- Zhou, J., Xue, D., Lei, L., Wang, L., Zhong, G., Liu, C., et al. (2019). Impacts of climate and land cover on soil organic carbon in the eastern Qilian Mountains, China. *Sustainability* 11:5790. doi: 10.3390/su11205790
- Zhu, M. L., Gao, H. Y., Xue, L. G., Zhang, J., and Wu, Y. M. (2015). Simulation and analysis of water balance process in Poyang Lake basin based on system dynamic approach. *Water Resour. Prot.* 31, 46–52.